NJC

ROYAL SOCIETY OF CHEMISTRY

PAPER

View Article Online
View Journal

Cite this: DOI: 10.1039/c9nj06187h

Chromogenic agents built around a multifunctional double-triazine framework for enzymatically triggered cross-linking under physiological conditions†

Hikaru Fujita, Yunlong Zhang, Zhiyuan Wu and Jonathan S. Lindsey *

An "A_2BC"-type bioconjugatable compound (**1**) that enables enzymatically triggered cross-linking chemistry has been designed and synthesized. The compound contains two indoxyl-glucoside units (A units), which upon action of a glucosidase undergo oxidative dimerization to form a water-insoluble indigoid dye. The other two moieties are azide (B, for click chemistry) and (C) a triazine-chloride or a coumarin dye; the former enables substitution with a nucleophile while the latter provides for ratiometric sensing of the extent of indigoid dye formation. A 7-component building block synthesis relies on successive substitution of 2 cyanuric chloride (2,4,6-trichloro-1,3,5-triazine) molecules with 5 other constituents (2A, B, C, and a piperazine–sulfobetaine moiety); the latter bear oligoethylene glycol (*i.e.*, PEG) or aminoalkyl tethers. The substitution reactions of cyanuric chloride proceed almost entirely at room temperature with control achieved by the order of nucleophile reactivity (aliphatic amine > phenol ≫ aliphatic alcohol) and the nature of a chosen base. Treatment of **1** with glucosidase under physiological conditions in aqueous solution gave an indigoid solution and a precipitate (~1 : 9 ratio) that were characterized by absorption spectrometry (including multicomponent analysis), dynamic light-scattering spectroscopy, and optical microscopy. Ratiometric absorption of the integral coumarin dye with the indigoid scaffold showed a low yield (3%) of oligomerization, which suggests future molecular designs might employ longer linkers and/or substituents with greater water solubility.

Received 13th December 2019,
Accepted 31st January 2020

DOI: 10.1039/c9nj06187h

rsc.li/njc

Introduction

The use of enzymes to trigger construction of molecular structures under physiological conditions has been relatively underexplored yet appears to afford immense opportunities in the life sciences. Such processes have afforded products across a broad range of molecular weight. In the low molecular weight regime, intramolecular cyclization following enzymatic cleavage has yielded fluorescent dyes.[1–6] In the medium molecular weight range, enzymatic unveiling of the cysteine thiol has triggered formation of cyanobenzothiazole–cysteine oligomers.[7–11] And for very large molecular products, enzyme-mediated cross-linking of polymers has afforded hydrogels.[12–16] The aforementioned examples chiefly entail covalent bond formation (related to covalent self-assembly[17]), yet non-covalent processes also have been exploited:[18,19] in enzyme-instructed self-assembly,[20] a peptide released by enzymatic cleavage assembles upon non-covalent interactions to form a nanostructure. Such covalently linked nanostructures suggest utility in diverse applications if suitable functionalities can be incorporated, such as bioconjugatable handles, fluorescent dyes, and/or ligands for biomolecules.

Among possible strategies for forming molecular scaffolds, indigogenic cross-linking[21,22] is promising for multiple reasons. First, the cross-linking can be triggered by enzymatic cleavage of a protecting group on an indoxyl precursor. Second, the cross-linking is covalent in nature and hence the reaction processes are essentially irreversible. Third, the cross-linking occurs in aqueous solution under physiological conditions without added reagents (other than the presence of O_2). Fourth, the indigo product (blue) affords a chromogenic readout in the red spectral region (~630 nm). And fifth, the indoxyl units can be attached to a wide variety of other molecular entities. Indigogenic cross-linking constitutes an oxidative homo-dimerization, and has been widely used in histochemistry for identification of the presence and locale of particular enzymes.[23] For broad use in life sciences applications, a generalized scaffold precursor is an A_2BC-tetrafunctionalized compound as shown in Fig. 1. The design

Department of Chemistry, North Carolina State University, Raleigh, NC 27695-8204, USA. E-mail: jlindsey@ncsu.edu

† Electronic supplementary information (ESI) available: ^{1}H and ^{13}C NMR spectra for all new compounds; and single-crystal X-ray data. CCDC 1902485 (**6-β**). For ESI and crystallographic data in CIF or other electronic format see DOI: 10.1039/c9nj06187h

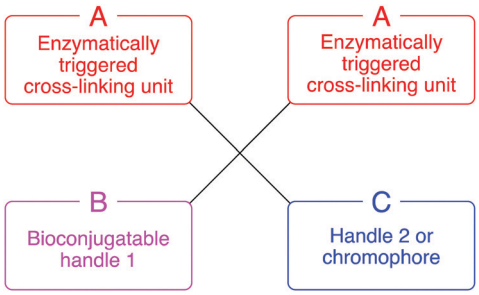

Fig. 1 A_2BC-molecular design with cross-linkable constituents and docking sites for forming molecular scaffolds.

includes two enzymatically cleavable indoxyl-protected cross-linking units (A_2), a bioconjugatable handle (B), and a molecular entity (C) such as a chromophore or reactive handle.

We have been working toward the synthesis of indoxyl-containing precursors for formation of molecular scaffolds. We first prepared compound **I**, which contains an indoxyl-glucoside and a strained cyclooctyne linked *via* two short PEG groups to a central triazine unit.[22] The glucoside can be cleaved by a glucosidase enzyme; the sulfobetaine attached to the central triazine imparts water solubility; and the cyclooctyne enables copper-free click chemistry to form the corresponding triazole. The rationale for the dibromoindoxyl moieties stems from systematic studies[22] of 15 indoxyl-glucoside substrates with β-glucosidase enzymes to identify molecular designs that (1) are water-soluble, (2) are compatible with enzymatic cleavage, (3) undergo facile indigoid dye formation under physiological conditions, (4) are synthetically accessible, and (5) support incorporation into larger architectures *via* bioconjugation chemistry. Compound **I** enables enzymatically triggered joining of two entities that are tethered *via* the respective cyclooctyne units. A related compound (**II**) contains two indoxyl-glucosides and affords a linear polymer upon glucosidase action (Chart 1).

The triazine-containing compounds **I** and **II** can be regarded as AB- and A_2-type architectures, respectively. The molecular design of an A_2BC-functionalized compound (**1**), which extends the designs of **I** and **II**, is shown in Chart 1. The structure contains a pair of alkoxy/amino-substituted triazines, two dibromoindoxyl β-glucosides (A_2), an azide (B), and an aminocoumarin dye (C). Compound **1** additionally bears a piperazine–sulfobetaine moiety as a linker between the two triazines to increase water solubility. In this paper, we describe the synthesis of **1** (and two early analogues thereof) and the reaction of **1** upon glucosidase action. The presence of the coumarin enables absorption ratiometry of the coumarin *versus* newly formed indigoid chromophores. The work provides a step toward the availability of scaffolds formed *in situ* for use in the life sciences.

Results and discussion

Synthesis of indoxyl-glucoside building blocks

The syntheses described herein rely on access to 5-hydroxyindoxyl-glucosides, both in the protected (*N*-acetyl, glucosyl *O*-peracetyl) and in the fully deprotected forms. The synthesis starts with 5-benzyloxyindole-3-carbaldehyde (**2**), which is commercially available in large quantity. Several forays into this chemistry over the years have been reported albeit with incomplete characterization and yield data. Here we describe in full these valuable transformations.

Treatment of indole **2** with acetic anhydride in the presence of triethylamine and a catalytic amount of 4-dimethylaminopyridine (DMAP) afforded the *N*-acetylated indole **3** (Scheme 1). Compound **3** was reported previously by Andreani *et al.*[24] with characterization by IR and ^{1}H NMR spectroscopy, but without yield information. The Baeyer–Villiger oxidation (known for the methoxy analogue)[25] of **3** afforded **4** in low yield (32%), but **3** was recovered in 42% yield and recycled. Compound **4** is displayed here in the keto rather than enol form. The synthesis of **4** *via* independent routes was reported previously by Nenitzescu and Raileanu[26] (with yield, mp and combustion analysis data); by Nimtz and Häfelinger[27] (with yield and mp data); and by Jautelat *et al.*[28] (without protocol or characterization data).

The glucosidation of **4** with acetobromo-α-D-glucose (**5**) was reported in acetonitrile containing potassium *tert*-butoxide at 0 °C for 4 h but without yield or characterization data.[29] Reaction of **4** and **5** with HgO/$HgBr_2$[30] in a mixture of toluene and nitromethane afforded stereoselective – but not exclusive – formation of the β-glucoside **6-β**. The ratio of **5** : **4** : HgO : $HgBr_2$ was 2.5 : 1 : 1 : 0.2; in other words a 2.5-fold quantity of acetobromo-α-D-glucose (**5**), a stoichiometric amount of HgO, and $HgBr_2$ at 20% relative to the glucosidation substrate **4**. Chromatography afforded the β- and α-diastereomers in isolated quantities of 6.98 and 0.44 g, respectively (16 : 1 ratio of **6-β** : **6-α**). The diagnostic feature in the ^{1}H NMR spectra to distinguish the two isomers stems from the anomeric proton (Fig. 2): a characteristic downfield resonance and smaller coupling constant is observed for the anomeric proton of the α-anomer (**6-α**, ~5.66 ppm, J = 3.5 Hz) *versus* that of the anomeric proton of the β-anomer (**6-β**, ~5.01 ppm, J = 6.0 Hz, in $CDCl_3$); the doublets arise by coupling with the adjacent proton at the 2-position.[31,32] Examination of the chromatographically separated β-isomer (**6-β**) revealed >99% stereochemical purity at the anomeric carbon (by comparison of the integrated areas of the ^{1}H NMR peaks at 5.01 and 5.66 ppm).

A single-crystal X-ray structure determination of **6-β** (recrystallized from hexanes/CH_2Cl_2) confirmed the assigned stereochemistry (Fig. 3). To our knowledge, only four single-crystal X-ray structures of 2-unsubstituted indoxyl compounds have been reported: 3-acetoxyindole,[33] *N*-(2-pyrimidinyl)-3-acetoxyindole,[34] and 4-bromo and 4,6-dibromo analogues of **6-β** that lack the benzyl group.[22] Hydrogenolytic debenzylation of **6-β** gave **7**[22] in 99% yield, whereas exhaustive removal of the acetyl groups by methanolysis followed by hydrogenolysis provided 5-hydroxyindoxyl-glucoside **8**[22] in 89% yield.

Synthesis of triazine-containing indoxyl-glucosides

Cyanuric chloride (2,4,6-trichloro-1,3,5-triazine) undergoes versatile derivatization with alcohols and amines[35–38] and here provides the source of two "molecular junctions" in the target architectures. The synthesis of two early analogues of **1** began

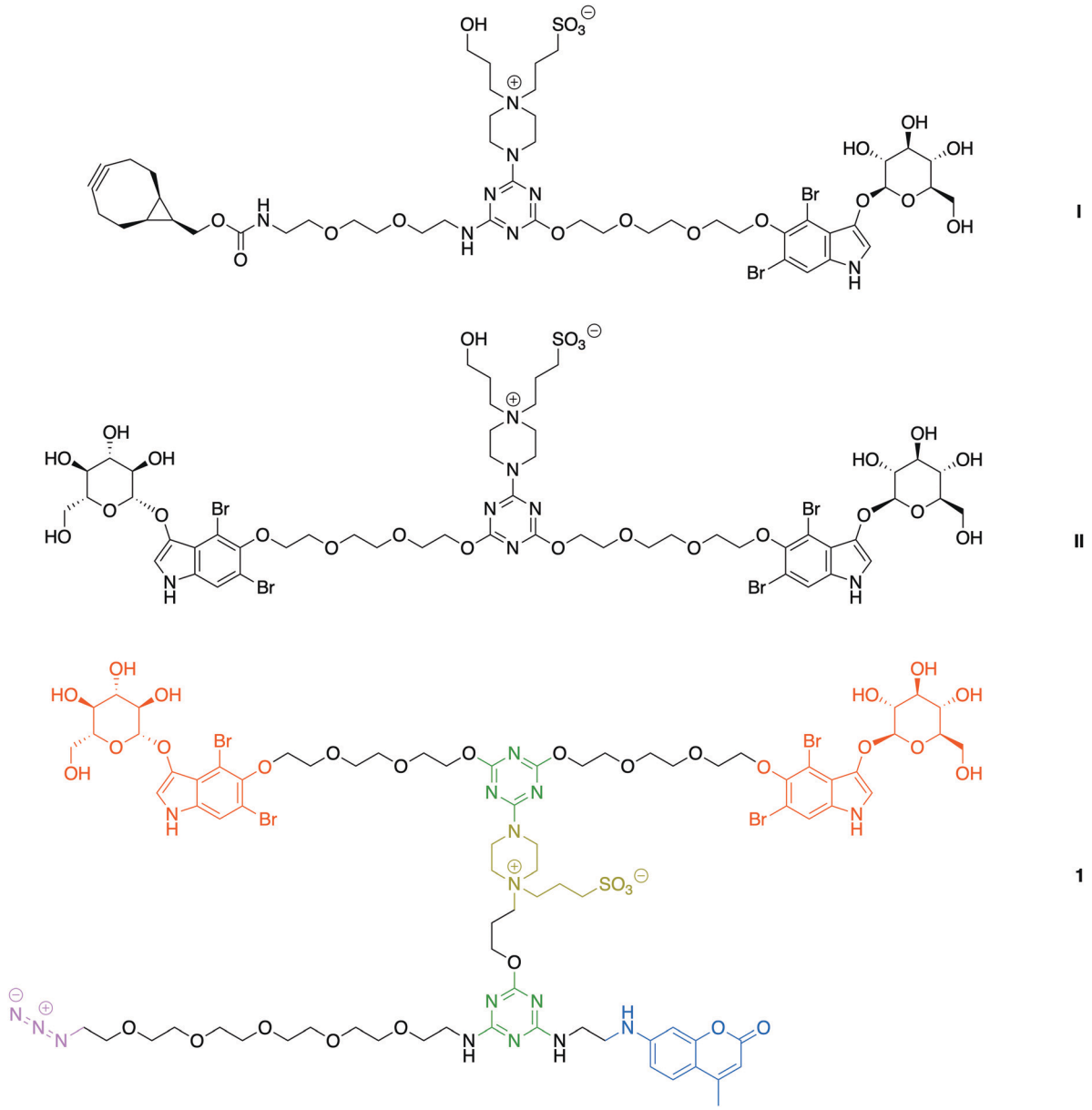

Chart 1 Prior indoxyl-containing constructs (**I**, **II**) and A_2BC-compound **1**.

by treatment of cyanuric chloride with 2 equivalents of indoxyl-glucoside **8** followed by tyramine to afford **9** in 56% yield (Scheme 2). Compound **9** is an A_2B-type architecture. Both reactions were carried out in acetonitrile/DMF (containing *N*,*N*-diisopropylethylamine) rather than the preferred solvent dichloromethane owing to solubility limitations.

A separate reaction of cyanuric chloride was carried out with the aliphatic alcohol *N*-(6-hydroxyhexyl)maleimide (**10**)[39] in the presence of the base 1,10-phenanthroline. Subsequent reaction with **9**, a trisubstituted triazine that bears a single phenol, in the presence of *N*,*N*-diisopropylethylamine gave **11** in 77% yield. Compound **11**, an A_2BC-architecture, contains two triazine units; the first bears two identical aryloxy substituents and one amino substituent, whereas the latter bears two distinct (aryloxy and alkoxy) substituents and one chlorine atom. Chromatographic purification of **9** and **11** was carried out on diol-functionalized silica (hydrophilic interaction chromatography), which affords intermediate polarity between bare silica and reversed phase derivatized silica.[40]

The synthesis of **9** and **11** without protecting groups illustrates an attractive feature of triazine chemistry. Control of successive substitutions in the triazine nucleus has traditionally been achieved by temperature variation: reaction with the first nucleophile at <0 °C, the second nucleophile at room temperature, and the third nucleophile at ≥ 60 °C.[37,38] The reactions here highlight the control of substitution both by order of reactants and by choice of base. The first reactant (**8**) employed with cyanuric chloride contains four aliphatic hydroxy groups, an indole NH, and a phenolic OH, yet reacts selectively at the phenolic OH; use of two equivalents of **8**

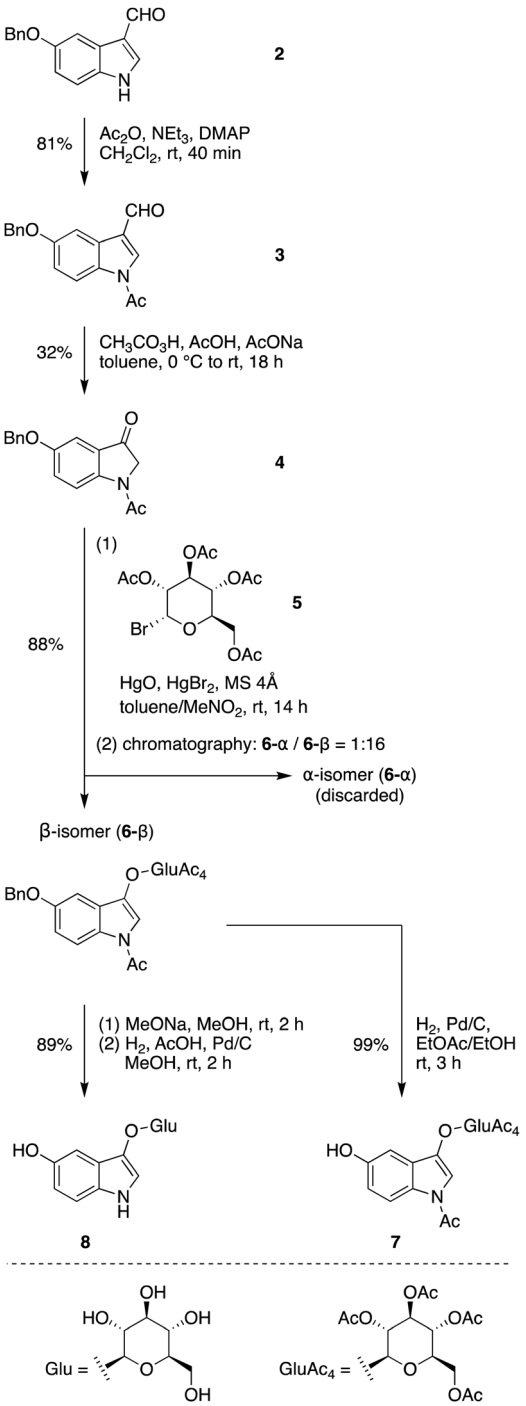

Scheme 1 Synthesis of 5-hydroxyindoxyl-glucosides.

causes displacement of two chlorides in cyanuric chloride. The second reactant (tyramine) contains a phenol and an aliphatic amine yet reacts selectively at the amine, causing substitution of the third chloride. In both reactions *N*,*N*-diisopropylethylamine (Hünig's base[41]) was employed: at 0 °C to room temperature for 2 h with phenol **8**, and at room temperature for 19 h with tyramine. The base 1,10-phenanthroline[42,43] was employed for the selective mono-substitution of cyanuric chloride with the aliphatic alcohol **10**, *versus* use of the stronger base

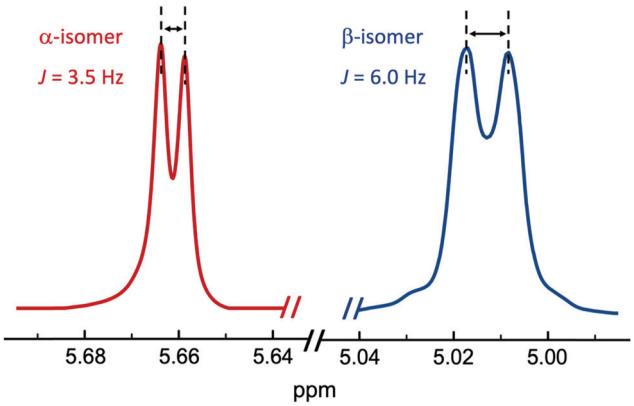

Fig. 2 ^{1}H NMR spectra (in $CDCl_3$ at room temperature) showing the signal from the anomeric proton in the α- *versus* β-anomers of **6**.

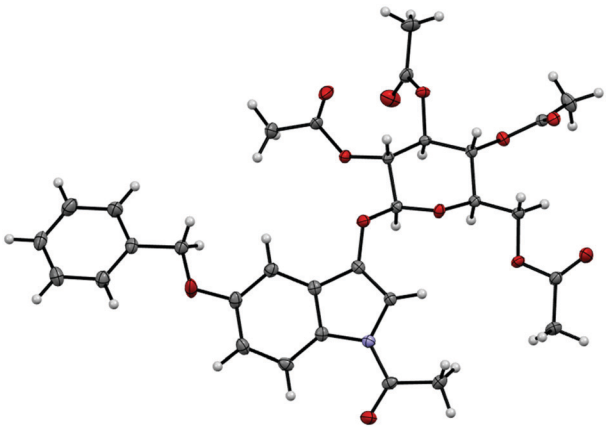

Fig. 3 ORTEP drawing of the single-crystal X-ray structure of **6-β**. All ellipsoids are contoured at the 50% level.

N,*N*-diisopropylethylamine for the second and third substitutions with phenol **9**. Compound **9** contains eight aliphatic hydroxy groups, two indole NH moieties, and a phenolic OH, yet reacts at the lone phenol to give the desired product **11** in good yield.

Ultimately, we found that **9** did not form the corresponding indigoid dye upon treatment with β-glucosidase. While **9** and **11** were attractive from the standpoint of synthesis given the ability to derivatize the phenolic OH of the indoxyl-glucoside without use of protective groups, the reaction with a β-glucosidase was *sine qua non* in the molecular design. Accordingly, we moved to the design of a more suitable architecture.

Compound **1** was designed with the following changes *versus* **9** and **11**. First, longer linkers were inserted between the triazine nucleus and the two indoxyl-glucoside moieties to facilitate indigogenic triggering by a β-glucosidase. Second, a piperazine–sulfobetaine unit was incorporated to increase water solubility. Third, a coumarin dye was included for ratiometric colorimetry. Fourth, an azide unit was included for click chemistry. And fifth, a 4,6-dibromoindoxyl unit was employed because we subsequently found[22] that the yield of indigoid dye formation is enhanced by the presence of the bromine atoms.

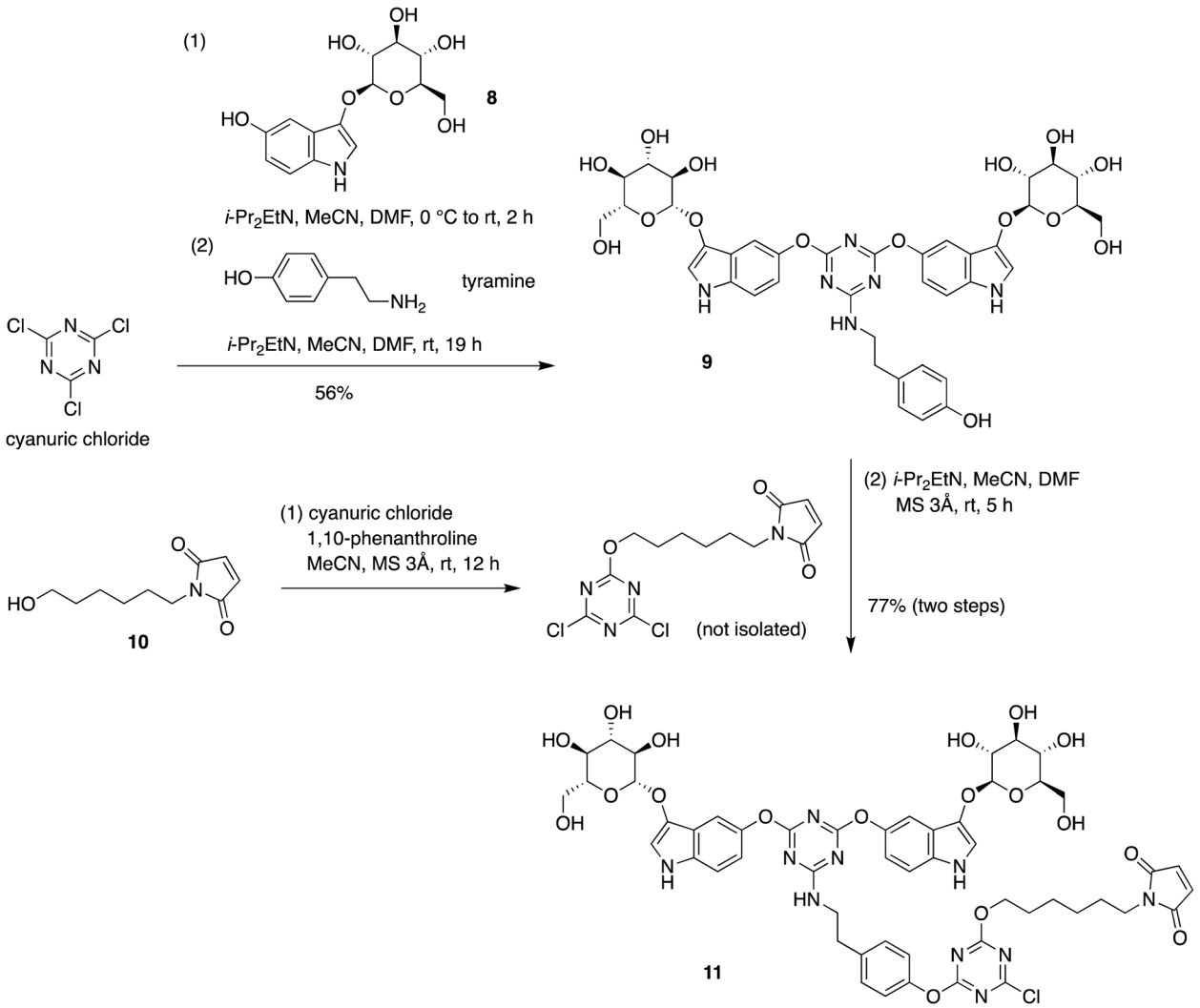

Scheme 2 Protecting group-free synthesis of an A_2BC-construct.

The synthesis began with 4,6-dibromoindoxyl-glucoside **12**, which bears a short hydroxy-terminated PEG linker along with acetyl protecting groups for the glucosyl alcohols and the indole nitrogen (Scheme 3). Here, protecting groups are required because an aliphatic (PEG) alcohol is the nucleophile (*versus* the phenol in the synthesis of **9** and **11**). The reaction of aliphatic alcohol **12** and cyanuric chloride was carried out to afford the corresponding dialkoxy-substituted triazine. Subsequent reaction with the piperazine–sulfobetaine **13**,[22] which bears amine and alcohol substituents, afforded **14** in 29% yield in 2 steps from cyanuric chloride, as described previously.[22] The reactions employed a series of bases including pempidine[22,44] to promote double-substitution of cyanuric chloride with the aliphatic alcohol **12**; *N*,*N*-diisopropylethylamine and methanol to cause *N*-acetyl cleavage; and 2,6-lutidine[43] to promote amination with the sulfobetaine-substituted piperazine **13**.[22]

Selective substitution[43] of one of three chlorides in cyanuric chloride by aliphatic alcohol **14** was carried out in the presence of 1,10-phenanthroline at room temperature (Scheme 3). Subsequently, azido-PEG_5-amine **15** was added to the reaction mixture to displace the second chloride. After the solvent was changed to DMF, the third substitution was carried out with the resulting chloro-triazine intermediate **16** (without isolation) and amino-coumarin **17**[45] in the presence of triethylamine at room temperature to afford **18** (39% yield from **14**). Treatment of **18** with K_2CO_3 in methanol caused exhaustive removal of the glucosyl *O*-acetyl groups and gave **1** in quantitative yield.

All new compounds were characterized by accurate-mass measurement as well as by ^1H and ^{13}C NMR spectroscopy. A noteworthy feature of the tri-substituted triazine-containing compounds here is slow C–N bond rotation between the triazine ring and an attached alkylamino (RHN–) group. The phenomenon of hindered rotation in amino-substitute triazines is known,[46–50] and tautomers have also been proposed.[46] Three cases are germane here (Fig. 4):

(1) For a triazine compound that bears two identical substituents (X) and an alkylamino group (**III**, exemplified by **9** and **11**), rotational isomers are not possible; however, distinguishable signals in the NMR spectrum are possible because the two X substituents experience non-equivalent environments with

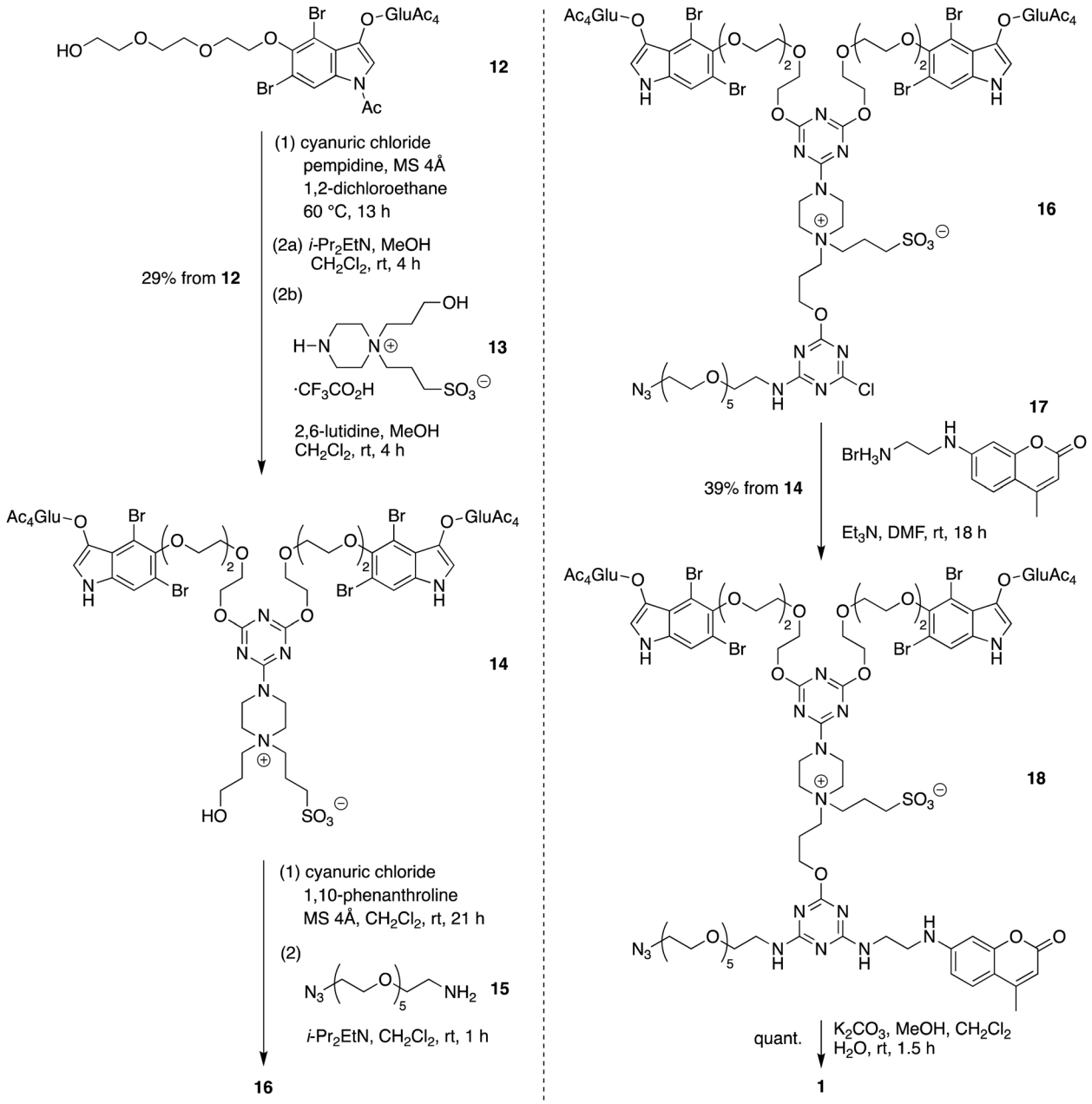

Scheme 3 Synthesis of **1** bearing indoxyl-glucoside, coumarin, and azide groups.

respect to the orientation of the substituents on the attached nitrogen atom. For example, in the case of **9**, 7 pairs of close ^{13}C NMR signals were observed from the indole moieties: (114.4, 115.0); (117.3, 117.5); (121.6, 121.7); (130.7, 131.0); (133.05, 133.15); (139.18, 139.21); and (146.5, 146.8). Three signals (169.3, 174.1, and 174.6 ppm) also were observed indicating the non-equivalent environment of the two C–O carbons in the triazine. Seven signals near 170 ppm were observed in the ^{13}C NMR spectrum of **11**; the signals were not assignable but are believed to stem from the $(ArO)_2(RNH)_1$-substituted triazine, the (Ar′O)(R′O)(Cl)-substituted triazine, and the maleimide.

(2) For a triazine compound that bears two different substituents (X and Y) and one alkylamino group (exemplified by **16**), a pair of rotational isomers (*i.e.*, rotamers **IVa** and **IVb**) is possible.

(3) For a triazine compound that bears two nonidentical alkylamino groups (exemplified by **18** and **1**), four rotamers (**Va–Vd**) are possible. Although evidence for the presence of rotamers was not very strong in the NMR spectra of **18** and **1**, slow C–N bond rotation was suggested by the following observations: (1) weak, multiple ^{13}C NMR signals from triazines at 165–170 ppm for **18** and for **1**; (2) split ^{1}H NMR signals from the aminocoumarin dye in **1**, such as signals at 5.877 and 5.894 ppm assigned to 3-H (which are not a doublet), and singlets from two indoxyls (7.208 and 7.548 ppm) that are spatially removed from the triazine; and (3) broad signals in

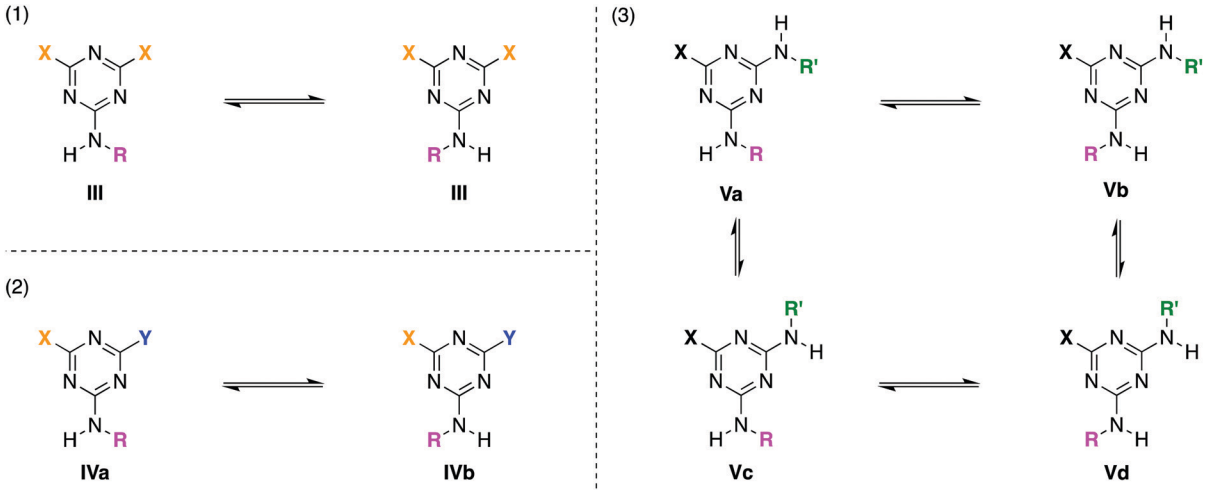

Fig. 4 Conformational interconversion due to hindered C–N bond rotation in triazines bearing alkylamino groups (possible tautomers[46] are not shown).

the ^{1}H NMR spectrum of **18**. While the presence of multiple peaks complicates interpretation of the NMR spectra of aminotriazines, the underlying phenomenon is established and readily understandable.

Indigoid oligomers of compound 1

The oligomerization of compound **1** was examined by treatment with the enzyme β-glucosidase. The reaction mixture contained a 250-fold ratio of **1** (50 μM) to β-glucosidase (200 nM) in a 2 mL reaction volume. The reaction mixture was only faintly blue after 5 h of incubation, but centrifugation afforded a blue precipitate. By visual inspection (Fig. 5, panel A), the yield of precipitate was low in comparison with our previously reported enzymatic treatment of compound **I**.[22] Multiple additions of β-glucosidase (to reach ∼1 μM total after 8 h) and longer incubation times (10 h or 24 h) were examined but no increase in solution intensity or precipitate was observed. For the samples after 5 h of incubation, the precipitates suspended in H_2O were screened by optical microscopy (Fig. 5, panel B) and dynamic light-scattering (DLS) spectroscopy (Fig. 5, panel C). The aggregates were between 100 and 1000 nm in size as measured by DLS analysis, which is consistent with the images obtained by optical microscopy (∼1 μm).

Quantitation of the indigogenic compounds in the precipitate and supernatant was carried out by absorption spectrometry (Fig. 5, panel D and E). For absorption spectrometry, the precipitate was dissolved in DMF. For consistent measurement, the supernatant was lyophilized, and the resulting residue was then taken up in DMF. Upon absorption spectrometry, multicomponent analysis (MCA)[51] was essential due to the overlapping absorption of indigo and coumarin at 362 nm, the peak wavelength for the coumarin. Spectral deconvolution relied on knowledge of the molar absorption coefficient at 362 nm of the coumarin (ε_{cou362} = 2.0 × 10^4 M^{-1} cm^{-1}, measured in DMF) and the indigo model compound **19**[22] shown in Chart 2 (ε_{ind362} = 0.81 × 10^4 M^{-1} cm^{-1}, measured in DMSO/H_2O, v/v = 2/1); and the molar absorption coefficient of **19** at 630 nm (ε_{ind630} = 2.6 × 10^4 M^{-1} cm^{-1}, measured in DMSO/H_2O, v/v = 2/1). (The coumarin does not absorb at 630 nm.) The residual upon MCA was smaller than any of the components, as required for accurate analysis.[52] In this manner, the precipitate was found to be composed of 51.6 nmol of coumarin and 2.8 nmol of indigoid dye, whereas the supernatant was composed of 11.1 nmol of coumarin and 0.3 nmol of indigoid dye.

The results obtained from the above analysis imply the following: (1) the total quantity of indigoid dye (3.1 nmol) corresponds to a yield of 3.1%; (2) the indigoid dye in the precipitate (2.8 nmol) is ∼9 times greater than that in the supernatant (0.3 nmol); (3) the total quantity of compound added (100 nmol) exceeds the total amount of coumarin calculated by MCA (62.7 nmol). This latter observation may stem from experimental error, loss on handling, and/or inaccuracy of the molar absorption coefficients of the indigoid dye in DMF employed in the MCA method. Regardless, the extent of oligomerization was low, which may stem from toxicity of the substrate to the β-glucosidase, linkers that are still too short, and/or aggregation of **1** prior to or during the course of enzymatic action. Examination of further molecular designs is required to better understand the origin of this result.

Outlook

The work described herein is aimed at developing the ability to create molecular scaffolds upon enzymatic action under physiological conditions. A long-term objective is to exploit such scaffolds for diverse applications in the life sciences ranging from molecular imaging and diagnostics to molecular brachytherapy and other therapeutic interventions. The challenges are multifold and encompass the nature of the cross-linking units, the choice of target enzyme and companion enzymatically cleavable groups, and composition of other units that are to be included in the target molecular scaffold. An underlying challenge concerns the

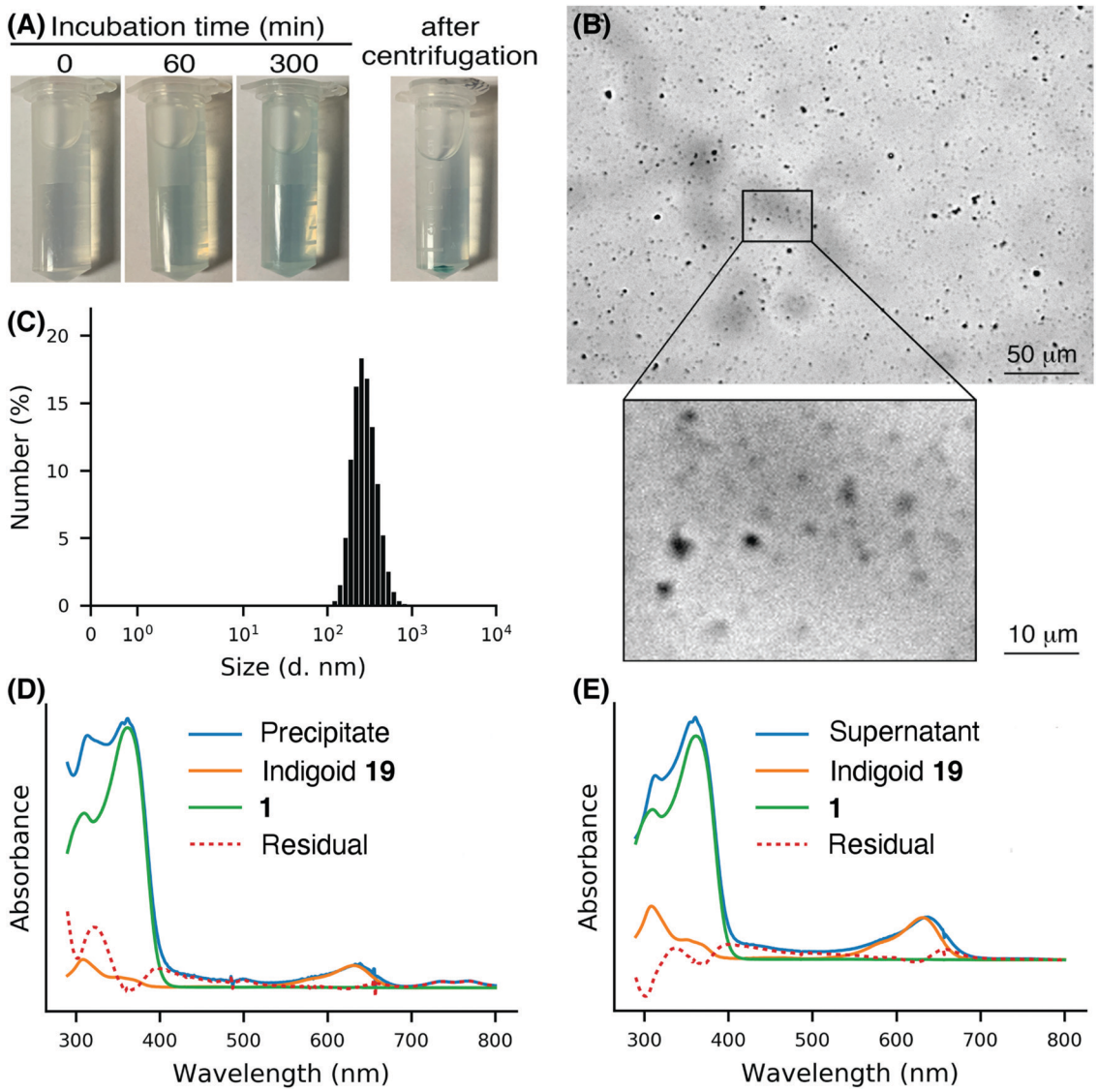

Fig. 5 The oligomerization of compound **1** upon enzymatic digestion with β-glucosidase. (A) Photographs of the reaction samples in a 300 min time course. (B) Optical microscopic image (×40) of the precipitate suspended in H_2O. (C) DLS analysis of the precipitate suspended in H_2O. (D) Absorption spectral MCA of the precipitate (dissolved in DMF). (E) Absorption spectral MCA of the supernatant (in DMF).

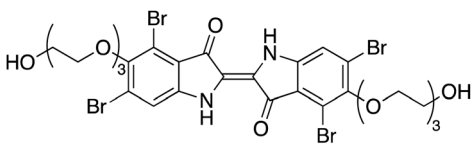

19

Chart 2 Indigoid dye model compound.[22]

method of synthesis. The results herein show that triazine chemistry is well suited for synthesis of architecturally and compositionally rich target compounds beginning with diverse building blocks; indeed, the triazine nucleus forms a type of molecular junction for attaching diverse constituents. The constituents incorporated here include indoxyl-glucosides, a coumarin dye, azide and chloro-triazine handles, PEG linkers, and piperazine–sulfobetaine linkers. Each such building block bears a single phenol, a single aliphatic amine, or a single unprotected aliphatic alcohol. The order of reactivity toward triazine-chloride displacement is aliphatic amine > phenol ≫ aliphatic alcohol. The phenol is sufficiently reactive with cyanuric chloride to enable use without protection of the accompanying (aliphatic) glucosyl alcohol and indole NH moieties; by the same token, an aliphatic amine reacts preferentially in the presence of an unprotected phenol.

The presence of an integral chromophore, such as the coumarin here, enables ratiometric analysis of the extent of indigogenesis upon enzymatic removal of the glucosyl groups from the two indoxyl moieties. We note that such ratiometric analysis is not necessary for chemistry experiments alone, given that the absorption due to the indigoid dye can be assessed directly and quantitatively. On the other hand, ratiometric

analysis is potentially quite valuable for studies in cells or tissues, where spectral imaging can be exploited to determine the extent of oligomerization. Such studies *in vivo* likely will require new molecular designs wherein the substrates afford higher water solubility and a higher yield of oligomerization to form the desired scaffold.

Experimental section

General methods

Commercial compounds were used as received unless noted otherwise. All solvents were reagent grade and were used as received unless noted otherwise. The CH_2Cl_2 employed in reactions was commercial anhydrous grade. $CHCl_3$ was stabilized with amylenes. Na_2SO_4 was anhydrous. Known compounds **8**,[22] **10**,[39] **12–14**,[22] and **17**[45] were prepared as described in the literature. Column chromatography was carried out using silica gel (40 μm) or diol-functionalized silica gel (40–63 μm). ^{1}H NMR and ^{13}C NMR spectra were collected at room temperature unless noted otherwise. Chemical shifts for ^{1}H NMR spectra are reported in parts per million (δ) relative to tetramethylsilane or a solvent signal [$(CD_3)_2SO$, δ = 2.50 ppm; CD_3OD, δ = 3.31 ppm]. Chemical shifts for ^{13}C NMR spectra are reported in parts per million (δ), and spectra were calibrated by using solvent signals [$CDCl_3$, δ = 77.16 ppm; $(CD_3)_2SO$, δ = 39.52 ppm; CD_3OD, δ = 49.00 ppm].[53]

Bases

Five organic bases were used as part of the chloro-triazine substitution reactions. The pK_a value of the conjugate acid of a given base in water is listed in parentheses as follows: 1,10-phenanthroline (4.96),[54] 2,6-lutidine (5.77),[55] triethylamine (10.74),[56] pempidine (1,2,2,6,6-pentamethylpiperidine, 11.25),[56] and *N*,*N*-diisopropylethylamine (11.44).[57]

Cyanuric chloride

Cyanuric chloride was recrystallized from hexanes/CH_2Cl_2 or hexanes/$CHCl_3$ and stored at −5 °C or −20 °C prior to use. Cyanuric chloride is soluble in CH_2Cl_2 or $CHCl_3$ whereas the hydrolyzed products are insoluble. The addition of CH_2Cl_2 or $CHCl_3$ (stabilized with amylenes) to pure cyanuric chloride immediately affords a clear solution. When clouding was found, the insoluble precipitate was removed by filtration, and the resulting filtrate was treated with hexanes to recrystallize the cyanuric chloride.

Reactions with cyanuric chloride require appropriate attention to detail. Cyanuric chloride is sufficiently electrophilic to react (even at 0 °C) with Et_3N, i-Pr_2EtN, DMF (solvent), or DMSO (solvent). Such bases and solvents were employed only with nucleophiles of sufficient reactivity (*e.g.*, amines, phenols). On the other hand, cyanuric chloride does not react with the bases 1,10-phenanthroline and pempidine at room temperature, which are well suited to facilitate selective substitution with aliphatic alcohols.

Synthetic compounds

1-Acetyl-5-(benzyloxy)-1*H*-indole-3-carbaldehyde (3). 4-Dimethylaminopyridine (104.9 mg, 0.858 mmol) was added to a suspension of **2** (21.57 g, 85.8 mmol), triethylamine (23.9 mL, 171 mmol), and Ac_2O (16.2 mL, 171 mmol) in CH_2Cl_2 (215 mL) at room temperature. After 40 min, the reaction mixture was washed with aqueous HCl (2 M, 200 mL), saturated aqueous $NaHCO_3$ (100 mL), and brine (100 mL). The organic layer was dried (Na_2SO_4) and filtered. The filtrate was concentrated and subjected to chromatography [silica, CH_2Cl_2/ethyl acetate (40 : 1)] to afford a pale brown solid (20.44 g, 81%): mp 120–121 °C; ^{1}H NMR (400 MHz, $CDCl_3$) δ 2.58 (s, 3H), 5.08 (s, 2H), 7.04 (d, J = 8.0 Hz, 1H), 7.20–7.60 (m, 5H), 7.75 (s, 1H), 7.82 (s, 1H), 8.19 (d, J = 8.0 Hz, 1H), 9.99 (s, 1H); ^{13}C NMR (100 MHz, $CDCl_3$) δ 23.5, 70.4, 105.1, 116.3, 117.2, 122.2, 127.0, 127.7, 128.0, 128.6, 130.9, 135.6, 136.9, 156.8, 168.3, 185.6; ESI-MS obsd 294.1126, calcd 294.1125 [$(M + H)^+$, M = $C_{18}H_{15}NO_3$].

1-Acetyl-5-(benzyloxy)indolin-3-one (4). Peracetic acid (32 wt% solution in acetic acid, 17.4 mL, 73 mmol) was added to a suspension of **3** (21.5 g, 73.3 mmol) and sodium acetate (12.0 g, 146 mmol) in toluene (293 mL) at 0 °C. The reaction mixture was stirred at 0 °C for 30 min followed by room temperature for 18 h. The reaction mixture was quenched by the addition of aqueous $Na_2S_2O_3$ (10%, 100 mL) and then filtered through Celite. The filtrate was washed with saturated aqueous $NaHCO_3$ (200 mL) and brine (100 mL), dried (Na_2SO_4), and filtered. The filtrate was concentrated and subjected to chromatography [silica, CH_2Cl_2/ethyl acetate (25 : 1)] to afford recovered **3** (8.94 g, 42%) and the title compound as a pale yellow solid (6.61 g, 32%): mp 163–164 °C; ^{1}H NMR (300 MHz, $CDCl_3$) δ 2.26 (s, 3H), 4.24 (s, 2H), 5.04 (s, 2H), 7.17 (d, J = 2.1 Hz, 1H), 7.26–7.46 (m, 6H), 8.46 (d, J = 9.3 Hz, 1H); ^{13}C NMR (75 MHz, $CDCl_3$) δ 24.0, 56.6, 70.5, 105.8, 119.8, 125.7, 126.8, 127.6, 128.3, 128.7, 136.2, 148.8, 155.6, 167.6, 194.5; ESI-MS obsd 282.1125, calcd 282.1125 [$(M + H)^+$, M = $C_{17}H_{15}NO_3$].

1-Acetyl-5-benzyloxy-1*H*-indol-3-yl 2,3,4,6-tetra-*O*-acetyl-β-D-glucopyranoside (6-β). A sample of $HgBr_2$ (0.937 g, 2.60 mmol) was added to a mixture of **4** (3.657 g, 13.0 mmol), acetobromo-α-D-glucose (**5**, 10.69 g, 26.0 mmol), HgO (2.816 g, 13.0 mmol), powdered molecular sieves 4 Å (26.0 g), and toluene/$MeNO_2$ (2 : 1, 130 mL) at room temperature. After 11 h, acetobromo-α-D-glucose (2.673 g, 6.50 mmol) was added. After 3 h, the reaction mixture was treated with pyridine (3.1 mL, 39 mmol) and filtered. The filtrate was concentrated and subjected to chromatography [silica, hexanes/acetone (7 : 3)] to afford **6-β** as a white solid (6.98 g, 88%) and **6-α** as a yellow oily solid (0.44 g, 5.5%). Data for **6-β**: mp 146–149 °C; ^{1}H NMR (700 MHz, $CDCl_3$) δ 2.05 (s, 3H), 2.06 (s, 3H), 2.07 (s, 3H), 2.08 (s, 3H), 2.58 (s, 3H), 3.83–3.89 (m, 1H), 4.22–4.30 (m, 2H), 5.01 (d, J = 6.0 Hz, 1H), 5.07–5.15 (m, 2H), 5.15–5.22 (m, 1H), 5.28–5.35 (m, 2H), 7.01 (s, 1H), 7.06 (d, J = 9.0 Hz, 1H), 7.11 (br s, 1H), 7.30–7.36 (m, 1H), 7.36–7.43 (m, 2H), 7.43–7.48 (m, 2H), 8.33 (br s, 1H); ^{13}C NMR (100 MHz, $CDCl_3$) δ 20.65, 20.68, 20.8, 23.8, 62.1, 68.3, 70.6, 71.2, 72.5, 72.6, 100.8, 101.7, 110.4, 115.7, 117.7, 125.0, 127.6, 128.1, 128.5, 128.7, 137.0, 141.4, 155.7, 167.9, 169.3, 169.5, 170.2, 170.6; ESI-MS obsd 612.2071, calcd 612.2076 [$(M + H)^+$, M = $C_{31}H_{33}NO_{12}$]. Suitable crystals for X-ray analysis

were obtained by recrystallization (hexanes/CH_2Cl_2). Data for **6-α**: ^{1}H NMR (700 MHz, $CDCl_3$) δ 2.06 (s, 3H), 2.07 (s, 3H), 2.08 (s, 3H), 2.08 (s, 3H), 2.55 (s, 3H), 4.12–4.16 (m, 1H), 4.25–4.28 (m, 2H), 5.08 (dd, J = 10, 3.5 Hz, 1H), 5.16 (d, J = 3.7, 1H), 5.20 (t, J = 10 Hz, 1H), 5.66 (d, J = 3.5, 1H), 5.76 (t, J = 10 Hz, 1H), 7.06–7.17 (m, 3H), 7.31–7.36 (m, 1H), 7.38–7.43 (m, 2H), 7.47–7.52 (m, 2H), 8.36 (br s, 1H).

2,4-Bis[3-(β-D-glucopyranosyloxy)-1*H*-indol-5-yloxy]-6-[2-(4-hydroxyphenyl)ethylamino]-1,3,5-triazine (9). *N*,*N*-Diisopropylethylamine (87.1 μL, 0.500 mmol) was added to a suspension of cyanuric chloride (36.9 mg, 0.200 mmol) and **8** (130.7 mg, 0.420 mmol) in MeCN (1.00 mL) at 0 °C. After 10 min, DMF (0.40 mL) was added at 0 °C. Then the reaction mixture was allowed to warm to room temperature and stirred for 2 h. Tyramine (30.2 mg, 0.220 mmol) and *N*,*N*-diisopropylethylamine (69.7 μL, 0.400 mmol) were added. After 19 h, the reaction mixture was treated with AcOH (23 μL, 0.40 mmol) and concentrated under reduced pressure. Column chromatography [diol-functionalized silica, CH_2Cl_2/MeOH (6 : 4)] followed by washing with H_2O afforded a pale yellow solid (94.1 mg, 56%): ^{1}H NMR (400 MHz, CD_3OD) δ 2.31–2.52 (m, 2H), 3.06 (t, J = 7.8 Hz, 2H), 3.05–3.17 (m, 1H), 3.24–3.56 (m, 7H), 3.62–3.78 (m, 2H), 3.78–3.96 (m, 2H), 4.64 (d, J = 8.0 Hz, 1H), 4.68 (d, J = 7.6 Hz, 1H), 6.35–6.48 (m, 4H), 6.90 (dd, J = 2.0, 8.8 Hz, 1H), 6.94 (dd, J = 2.0, 8.8 Hz, 1H), 7.18 (s, 1H), 7.24 (s, 1H), 7.29 (d, J = 8.8 Hz, 1H), 7.34 (d, J = 8.8 Hz, 1H), 7.51 (d, J = 2.0 Hz, 1H), 7.56 (d, J = 2.0 Hz, 1H); ^{13}C NMR (100 MHz, CD_3OD) δ 35.6, 44.4, 62.5, 62.6, 70.0, 71.3, 71.5, 75.0, 77.9, 78.0, 78.2, 106.1, 111.0, 112.9, 114.4, 115.0, 116.1, 117.3, 117.5, 121.6, 121.7, 130.7, 131.0, 133.05, 133.15, 139.18, 139.21, 146.5, 146.8, 156.4, 169.3, 174.1, 174.6, ESI-MS obsd 835.2756, calcd 835.2781 [$(M + H)^+$, $M = C_{39}H_{42}N_6O_{15}$].

2,4-Bis[3-(β-D-glucopyranosyloxy)-1*H*-indol-5-yloxy]-6-[2-(4-(2-(6-maleimidohexyloxy)-6-chloro-1,3,5-triazin-4-yloxy)phenyl)-ethylamino]-1,3,5-triazine (11). Cyanuric chloride (16.6 mg, 0.0900 mmol) was added to a suspension of hydroxyhexylmaleimide **10** (21.3 mg, 0.108 mmol), 1,10-phenanthroline (27.0 mg, 0.150 mmol), and molecular sieves 3 Å (45.0 mg) in MeCN (450 μL) at room temperature. After 12 h, **9** (50.1 mg, 0.0600 mmol), DMF (180 μL), and *N*,*N*-diisopropylethylamine (31.4 μL, 0.180 mmol) were added. After 5 h, the reaction mixture was subjected to chromatography [diol-functionalized silica, CH_2Cl_2/MeOH (17 : 3)] to afford a yellow solid (53.0 mg, 77%): ^{1}H NMR (400 MHz, CD_3OD) δ 1.18–1.40 (m, 4H), 1.44–1.59 (m, 2H), 1.60–1.74 (m, 2H), 2.47–2.66 (m, 2H), 3.08–3.53 (m, 12H), 3.66 (dd, J = 5.2, 12.0 Hz, 1H), 3.72 (dd, J = 5.2, 12.0 Hz, 1H), 3.81 (dd, J = 2.4, 12.0 Hz, 1H), 3.90 (dd, J = 2.4, 12.0 Hz, 1H), 4.30 (t, J = 6.8 Hz, 2H), 4.57 (d, J = 7.2 Hz, 1H), 4.68 (d, J = 7.2 Hz, 1H), 6.66 (d, J = 8.4 Hz, 2H), 6.76 (s, 2H), 6.82 (d, J = 8.4 Hz, 2H), 6.91 (dd, J = 2.0, 8.8 Hz, 1H), 6.97 (dd, J = 2.0, 8.8 Hz, 1H), 7.18 (s, 1H), 7.21 (s, 1H), 7.30 (d, J = 8.8 Hz, 1H), 7.34 (d, J = 8.8 Hz, 1H), 7.51 (d, J = 2.0 Hz, 1H), 7.57 (d, J = 2.0 Hz, 1H); ^{13}C NMR (100 MHz, CD_3OD/CD_3CN) δ 26.0, 27.1, 29.1, 29.2, 35.6, 38.4, 43.8, 62.5, 62.6, 70.6, 71.2, 71.3, 74.8, 74.9, 77.76, 77.80, 77.9, 78.0, 105.77, 105.80, 110.8, 110.9, 113.0, 114.1, 114.4, 117.4, 117.7, 118.3, 138.5, 139.0, 139.1, 146.4, 146.7, 151.2, 169.4, 172.6, 173.5, 173.6, 173.7, 174.0, 174.5; ESI-MS obsd 1143.3450, calcd 1143.3457 [$(M + H)^+$, $M = C_{52}H_{55}ClN_{10}O_{18}$].

2,4-Bis[1-(3-(2,3,4,6-tetra-*O*-acetyl-β-D-glucopyranosyloxy)-4,6-dibromo-1*H*-indol-5-yl)-1,4,7,10-tetraoxadec-10-yl]-6-[4-(3-(2-(1-azido-3,6,9,12,15-pentaoxoheptadecylamino)-4-[2-((4-methyl-2*H*-chromen-2-one-7-yl)amino)ethylamino]-1,3,5-triazin-6-yloxy)-propyl)-4-(3-sulfopropyl)piperazin-1-yl]-1,3,5-triazine (18). A sample of cyanuric chloride (4.4 mg, 0.024 mmol) was added to a suspension of **14** (37.6 mg, 0.020 mmol), 1,10-phenanthroline (9.0 mg, 0.050 mmol), and molecular sieves 4 Å (10 mg) in CH_2Cl_2 (100 μL) at room temperature. After 21 h, **15** (7.8 μL, 0.028 mmol) and *N*,*N*-diisopropylethylamine (10.5 μL, 0.060 mmol) were added. After 22 h, the reaction mixture was diluted with CH_2Cl_2 (2 mL), filtered, washed with aqueous citric acid (10%, 2 mL) and brine (2 mL), dried (Na_2SO_4), and filtered. The filtrate was concentrated under reduced pressure to afford the crude **16** (2,4-bis[1-(3-(2,3,4,6-tetra-*O*-acetyl-β-D-glucopyranosyloxy)-4,6-dibromo-1*H*-indol-5-yl)-1,4,7,10-tetraoxadec-10-yl]-6-[4-(3-(2-(1-azido-3,6,9,12,15-pentaoxoheptadecylamino)-4-chloro-1,3,5-triazin-6-yloxy)propyl)-4-(3-sulfopropyl)piperazin-1-yl]-1,3,5-triazine), which was used directly in the next step. Coumarin **17** (12.0 mg, 0.040 mmol), DMF (100 μL), and triethylamine (22 μL, 0.16 mmol) were added to the crude **16** at room temperature. After 18 h, the reaction mixture was diluted with CH_2Cl_2 (2 mL) and filtered. The filtrate was washed with aqueous citric acid (10%, 2 mL) and brine (2 mL), dried (Na_2SO_4), and filtered. The filtrate was concentrated under reduced pressure. Column chromatography [silica, CH_2Cl_2/MeOH (15 : 1 to 9 : 1) afforded a pale brown solid (19.4 mg, 39%): ^{1}H NMR ($CDCl_3$, 400 MHz, mixture of rotamers) δ 1.70–1.90 (m, 2H), 1.95–2.17 (m, 26H), 2.29 (s, 3H), 2.93 (br s, 2H), 3.10–4.60 (m, 73H), 4.81–4.98 (m, 2H), 5.05–5.40 (m, 6H), 5.73–6.05 (m, 3H), 6.38–6.65 (m, 2H), 6.88 (br s, 1H), 7.14 (s, 2H), 7.50–7.68 (m, 2H), 10.13 (br s, 2H); ^{13}C NMR ($CDCl_3$, 175 MHz, mixture of rotamers) δ 18.2, 18.7, 20.8, 21.2, 21.4, 36.9, 39.6, 39.8, 40.6, 40.7, 40.8, 43.0, 43.2, 43.3, 47.26, 47.32, 47.5, 50.8, 53.6, 56.4, 58.3, 62.0, 62.7, 67.1, 68.5, 69.2, 69.8, 70.1, 70.4, 70.6, 70.66, 70.71, 70.73, 70.9, 71.1, 72.0, 72.5, 73.1, 97.5, 101.3, 106.4, 108.48, 108.55, 109.9, 110.5, 111.8, 115.1, 115.7, 118.4, 125.6, 131.5, 136.5, 145.7, 152.1, 152.3, 153.7, 153.8, 156.0, 162.3, 166.4, 166.6, 166.8, 167.0, 167.2, 169.6, 169.7, 169.9, 170.3, 170.8, 171.7; ESI-MS obsd 1238.2465, calcd 1238.2484 [$(M + 2H)^{2+}$, $M = C_{96}H_{126}Br_4N_{16}O_{39}S$].

2,4-Bis[1-(3-(β-D-glucopyranosyloxy)-4,6-dibromo-1*H*-indol-5-yl)-1,4,7,10-tetraoxadec-10-yl]-6-[4-(3-(2-(1-azido-3,6,9,12,15-pentaoxoheptadecylamino)-4-[2-((4-methyl-2*H*-chromen-2-one-7-yl)-amino)ethylamino]-1,3,5-triazin-6-yloxy)propyl)-4-(3-sulfopropyl)-piperazin-1-yl]-1,3,5-triazine (1). K_2CO_3 (0.9 mg, 7 μmol) was added to a solution of **18** (15.9 mg, 6.4 μmol) in MeOH/$CHCl_3$ (4 : 1, 916 μL) at room temperature. After 30 min, H_2O (366 μL) was added. After 1.5 h, the reaction mixture was diluted with CH_2Cl_2 (2 mL), dried (Na_2SO_4), and passed through a pad of diol-functionalized silica [CH_2Cl_2/MeOH (2 : 1) as eluent]. The eluent was concentrated under reduced pressure to afford a pale yellow solid (13.7 mg, 100%): ^{1}H NMR ($CDCl_3$, 400 MHz, mixture of rotamers) δ 2.09 (br s, 2H), 2.15 (br s, 2H),

2.25–2.33 (m, 3H), 2.54–2.63 (m, 2H), 3.14 (t, J = 9.1 Hz, 2H), 3.18–4.43 (m, 76H), 4.64 (d, J = 7.3 Hz, 2H), 5.85–5.95 (m, 1H), 6.40–6.66 (m, 2H), 7.21 (s, 2H), 7.36–7.47 (m, 1H), 7.55 (s, 2H); ^{13}C NMR (DMSO-d_6, 175 MHz, mixture of rotamers) δ 17.9, 18.1, 20.8, 36.9, 47.3, 47.4, 48.6, 50.0, 52.9, 57.1, 57.2, 61.0, 66.5, 68.5, 68.8, 68.9, 69.3, 69.48, 69.54, 69.59, 69.64, 69.7, 69.8, 69.9, 70.0, 70.1, 72.4, 73.6, 76.9, 77.2, 103.4, 106.2, 107.5, 108.9, 110.5, 113.3, 114.9, 117.9, 126.0, 131.0, 137.4, 144.8, 152.4, 153.8, 153.86, 153.91, 155.7, 155.76, 155.80, 160.8, 160.9, 166.4, 166.7, 167.1, 169.8, 171.5; ESI-MS obsd 1070.2073, calcd 1070.2061 [$(M + 2H)^{2+}$, M = $C_{80}H_{110}Br_4N_{16}O_{31}S$].

Oligomerization study

Materials. DMF (HPLC grade) was purchased from Alfa Aesar. H_2O (molecular biology grade) for buffer preparation was purchased from Millipore Sigma. Compound **1** (5.6 mg) was dissolved in DMF (26 μL) to prepare a 100 mM stock solution. Sodium phosphate (Pi) buffer was prepared freshly at 10 mM, pH 7. The enzyme β-glucosidase from *Agrobacterium sp.* was purchased from MegaZyme and was dissolved in Pi buffer at 10 μM as the stock solution.

Molar absorption coefficients. The stock solution of compound **1** was diluted 1000-fold and 2000-fold with DMF to determine the molar absorption coefficients: ε_{310nm} = 1.37 × 10^4 M^{-1} cm^{-1}, ε_{362nm} = 2 × 10^4 M^{-1} cm^{-1}. The absorption coefficient of compound **1** in Pi buffer (containing 1–5% DMF and 1% DMSO) was not obtained due to aggregation.

Enzymatic treatment. To screen the oligomerization procedure of compound **1**, samples of Pi buffer (1859 μL), DMF (100 μL), β-glucosidase stock (40 μL) and compound **1** stock (1 μL) were mixed in a 2 mL Eppendorf tube. The resulting reaction mixture (2.0 mL) contained 50 μM of compound **1** (substrate) and 0.20 μM of β-glucosidase (enzyme). Three identical samples were prepared for different assays. For a control sample, 40 μL of Pi buffer was added as a replacement for the β-glucosidase stock solution. The tubes were incubated at 37 °C for 5 h, and pictures of the tubes were captured at 0, 15, 30, 60, 120, 180 and 300 min. After 300 min, the tubes were centrifuged at 20 000 × g for 10 min to isolate any precipitate from the supernatant. No precipitate was observed in the control sample.

In a study to assess whether the low yield of indigoid formation stemmed from insufficient enzyme, an additional aliquot (equaling ∼0.20 μM) of β-glucosidase was added to the reaction mixture every 2 h to give a total of ∼1 μM of β-glucosidase after 8 h. Other reactions were examined at longer reaction times (up to 24 h). Regardless, no change was observed in the yield of indigoid chromophores.

Analyses. Three samples were treated differently for the three assays: (1) for sample 1, the precipitate was dissolved in 100 μL of DMF for absorption analysis; (2) for sample 2, the precipitate was suspended in 100 μL of H_2O for optical microscopy; and (3) for sample 3, the precipitate was suspended in 1000 μL of H_2O for DLS analysis. The supernatant of sample 1 was freeze-dried under high vacuum, and the resulting residue was dissolved in 100 μL of DMF for absorption analysis. The absorption spectra of the DMF solutions of the precipitates and supernatants were employed for quantitation of indigoid and coumarin chromophores.

Optical microscopy of the suspended precipitate was carried out using a Zeiss Axio Observer Z1 inverted microscope with a 40× objective lens in the phase contrast mode. DLS spectroscopy was carried out with a Malvern Zetasizer Nano. Multicomponent analysis (MCA) was carried out using the software PhotochemCAD 3[51] with the following parameters: range, 290–700 nm; selected points, 362, 576 and 631 nm.

Conflicts of interest

Patent applications have been filed encompassing portions of this work for which all coauthors are coinventors.

Acknowledgements

The work was supported by NC State University. Accurate mass measurements were carried out in the Molecular Education, Technology, and Research Innovation Center (METRIC) at NC State University.

References

1 A. Romieu, *Org. Biomol. Chem.*, 2015, **13**, 1294–1306.
2 S. Debieu and A. Romieu, *Org. Biomol. Chem.*, 2015, **13**, 10348–10361.
3 S. Debieu and A. Romieu, *Org. Biomol. Chem.*, 2017, **15**, 2575–2584.
4 T. He, H. He, X. Luo, Y. Yang and Y. Yang, *Sci. Sin.: Chim.*, 2017, **47**, 945–954.
5 S. Debieu and A. Romieu, *Tetrahedron Lett.*, 2018, **59**, 1940–1944.
6 K. Renault, S. Debieu, J.-A. Richard and A. Romieu, *Org. Biomol. Chem.*, 2019, **17**, 8918–8932.
7 G. Liang, H. Ren and J. Rao, *Nat. Chem.*, 2010, **2**, 54–60.
8 Y. Yuan and G. Liang, *Org. Biomol. Chem.*, 2014, **12**, 865–871.
9 Y. Yuan, J. Zhang, M. Wang, B. Mei, Y. Guan and G. Liang, *Anal. Chem.*, 2013, **85**, 1280–1284.
10 X. Ai, C. J. H. Ho, J. Aw, A. B. E. Attia, J. Mu, Y. Wang, X. Wang, Y. Wang, X. Liu, H. Chen, M. Gao, X. Chen, E. K. L. Yeow, G. Liu, M. Olivo and B. Xing, *Nat. Commun.*, 2016, **7**, 10432.
11 M. Zhang and G. Liang, *Sci. China: Chem.*, 2018, **61**, 1088–1098.
12 J. Hu, G. Zhang and S. Liu, *Chem. Soc. Rev.*, 2012, **41**, 5933–5949.
13 L. S. M. Teixeira, J. Feijen, C. A. van Blitterswijk, P. J. Dijkstra and M. Karperien, *Biomaterials*, 2012, **33**, 1281–1290.
14 Q. Wei, M. Xu, C. Liao, Q. Wu, M. Liu, Y. Zhang, C. Wu, L. Cheng and Q. Wang, *Chem. Sci.*, 2016, **7**, 2748–2752.
15 X. Wang, S. Chen, D. Wu, Q. Wu, Q. Wei, B. He, Q. Lu and Q. Wang, *Adv. Mater.*, 2018, **30**, 1705668.

16 D. Wang, X. Yang, Q. Liu, L. Yu and J. Ding, *J. Mater. Chem. B*, 2018, **6**, 6067–6079.
17 J. S. Lindsey, *New J. Chem.*, 1991, **15**, 153–180.
18 Z. Feng, T. Zhang, H. Wang and B. Xu, *Chem. Soc. Rev.*, 2017, **46**, 6470–6479.
19 J. Mu, J. Lin, P. Huang and X. Chen, *Chem. Soc. Rev.*, 2018, **47**, 5554–5573.
20 J. Zhou and B. Xu, *Bioconjugate Chem.*, 2015, **26**, 987–999.
21 G. L. Mayers, *Drug Dev. Res.*, 2006, **67**, 94–106.
22 H. Fujita, J. Dou, N. Matsumoto, Z. Wu and J. S. Lindsey, *New J. Chem.*, 2020, **44**, 719–743.
23 J. A. Kiernan, *Biotech. Histochem.*, 2007, **82**, 73–103.
24 A. Andreani, A. Cavalli, M. Granaiola, M. Guardigli, A. Leoni, A. Locatelli, R. Morigi, M. Rambaldi, M. Recanatini and A. Roda, *J. Med. Chem.*, 2001, **44**, 4011–4014.
25 A. S. Bourlot, E. Desarbre and J. Y. Mérour, *Synthesis*, 1994, 411–416.
26 C. D. Nenitzescu and D. Raileanu, *Chem. Ber.*, 1958, **91**, 1141–1145.
27 M. Nimtz and G. Häfelinger, *Liebigs Ann. Chem.*, 1987, 765–770.
28 R. Jautelat, T. Brumby, M. Schäfer, H. Briem, G. Eisenbrand, S. Schwahn, M. Krüger, U. Lücking, O. Prien and G. Siemeister, *ChemBioChem*, 2005, **6**, 531–540.
29 G. L. Mayers, D. Lee and H.-L. Chin, US7615221B2, 2009.
30 L. R. Schroeder and J. W. Green, *J. Chem. Soc. C*, 1966, 530–531.
31 G. R. Periyannan, B. A. Lawrence and A. E. Egan, *J. Chem. Educ.*, 2015, **92**, 1244–1249.
32 J.-L. Giner, J. Feng and D. J. Kiemle, *J. Nat. Prod.*, 2016, **79**, 2413–2417.
33 D. K. Chakraborty, A. Mukhopadhyay and S. K. Talapatra, *Acta Crystallogr.*, 1991, **47**, 592–594.
34 L. Wang, X. Qu, Z. Li, C. Gu and S. Hu, *Chem. Res. Chin. Univ.*, 2016, **37**, 254–260.
35 C. Afonso, N. M. T. Lourenco and A. de Rosatella, *Molecules*, 2006, **11**, 81–102.
36 M. B. Steffensen, E. Hollink, F. Kuschel, M. Bauer and E. E. Simanek, *J. Polym. Sci., Part A: Polym. Chem.*, 2006, **44**, 3411–3433.
37 G. Blotny, *Tetrahedron*, 2006, **62**, 9507–9522.
38 K. Bretterbauer and C. Schwarzinger, *Curr. Org. Synth.*, 2012, **9**, 342–356.
39 K. A. Keller, J. Guo, S. Punna and M. G. Finn, *Tetrahedron Lett.*, 2005, **46**, 1181–1184.
40 P. Jandera, *Anal. Chim. Acta*, 2011, **692**, 1–25.
41 S. Hünig and M. Kiessel, *Chem. Ber.*, 1958, **91**, 380–392.
42 H. Fujita, N. Hayakawa and M. Kunishima, *J. Org. Chem.*, 2015, **80**, 11200–11205.
43 M. Kunishima, R. Asao, K. Yamada, M. Kitamura and H. Fujita, *J. Fluorine Chem.*, 2016, **190**, 68–74.
44 K. Ishihara, H. Kurihara and H. Yamamoto, *J. Org. Chem.*, 1993, **58**, 3791–3793.
45 Y. Shiraishi, S. Sumiya and T. Hirai, *Org. Biomol. Chem.*, 2010, **8**, 1310–1314.
46 H. E. Birkett, R. K. Harris, P. Hodgkinson, K. Carr, M. H. Charlton, J. C. Cherryman, A. M. Chippendale and R. P. Glover, *Magn. Reson. Chem.*, 2000, **38**, 504–511.
47 H. E. Birkett, J. C. Cherryman, A. M. Chippendale, J. S. O. Evans, R. K. Harris, M. James, I. J. King and G. J. McPherson, *Magn. Reson. Chem.*, 2003, **41**, 324–336.
48 M. Pintea, M. Fazekas, P. Lameiras, I. Cadis, C. Berghian, I. Silaghi-Dumitrescu, F. Popa, C. Bele, N. Plé and M. Darabantu, *Tetrahedron*, 2008, **64**, 8851–8870.
49 M. Fazekas, M. Pintea, P. Lameiras, A. Lesur, C. Berghian, I. Silaghi-Dumitrescu, N. Plé and M. Darabantu, *Eur. J. Org. Chem.*, 2008, 2473–2494.
50 E. Loeser and S. Babiak, *J. Chromatogr. A*, 2011, **1218**, 8672–8678.
51 M. Taniguchi, H. Du and J. S. Lindsey, *Photochem. Photobiol.*, 2018, **94**, 277–289.
52 Y. Zhang, R. Zhang, R.-A. Hughes, J. Dai, J. R. Gurr, P. G. Williams, E. S. Miller and J. S. Lindsey, *Phytochem. Anal.*, 2018, **29**, 205–216.
53 G. R. Fulmer, A. J. M. Miller, N. H. Sherden, H. E. Gottlieb, A. Nudelman, B. M. Stoltz, J. E. Bercaw and K. I. Goldberg, *Organometallics*, 2010, **29**, 2176–2179.
54 W. Robb and C. G. Nicholson, *S. Afr. J. Chem.*, 1978, **31**, 1–5.
55 H. C. Brown and B. Kanner, *J. Am. Chem. Soc.*, 1966, **88**, 986–992.
56 H. K. Hall Jr., *J. Am. Chem. Soc.*, 1957, **79**, 5444–5447.
57 T. Fujii, H. Nishida, Y. Abiru, M. Yamamoto and M. Kise, *Chem. Pharm. Bull.*, 1995, **43**, 1872–1877.

